

CLOSE ENCOUNTERS BETWEEN A NEUTRON STAR AND A MAIN-SEQUENCE STAR

Hyung Mok Lee

Department of Earth Sciences, Pusan University, Pusan 609-735, Korea

e-mail: hmlee@astrophys.es.pusan.ac.kr

Sungsoo S. Kim

Institute for Basic Sciences, Pusan University, Pusan 609-735, Korea; and

Department of Physics & Astronomy, University of California, Los Angeles, CA 90024, U. S. A.

e-mail: sskim@astrophys.es.pusan.ac.kr

and

Hyesung Kang

Department of Earth Sciences, Pusan University, Pusan 609-735, Korea

e-mail: kang@astrophys.es.pusan.ac.kr

Received _____; accepted _____

ABSTRACT

We have examined consequences of strong tidal encounters between a neutron star and a normal star using SPH as a possible formation mechanism of isolated recycled pulsars in globular clusters. We have made a number of SPH simulations for close encounters between a main-sequence star of mass ranging from 0.2 to 0.7 M_{\odot} represented by an $n=3/2$ polytrope and a neutron star represented by a point mass. The outcomes of the first encounters are found to be dependent only on the dimensionless parameter $\eta' \equiv (m/(m+M))^{1/2}(r_{\min}/R_{MS})^{3/2}(m/M)^{(1/6)}$, where m and M are the mass of the main-sequence star and the neutron star, respectively, r_{\min} the minimum separation between two stars, and R_{MS} the size of the main-sequence star. The material from the (at least partially) disrupted star forms a disk around the neutron star. If all material in the disk is to be accreted onto the neutron star's surface, the mass of the disk is enough to spin up the neutron star to spin period of 1 ms.

Subject headings: celestial mechanics – stellar dynamics – globular clusters: general – pulsars: general

1. INTRODUCTION

The cores of globular clusters have high stellar densities. Recent studies showed that the physical interactions between stars are main driving force in determining the dynamical evolution after the core collapse (e.g., Goodman 1988). The physical interactions include direct collisions between normal stars, tidal captures between a normal star and a compact star (neutron star or white dwarf), and formation of binaries via three-body processes.

Such interactions can lead to the formation of objects that are not common in low stellar environments. Indeed globular clusters reveal high abundance of X-ray binaries and short period pulsars. These systems are thought to be related to the physical interactions between stars. X-ray binaries can be formed either by tidal capture between a neutron star and a main-sequence star, or by the evolution of primordial binary.

Another observational evidence for the high abundance of the physical interactions in clusters is the enhancement of short-period pulsars. A large number of short period pulsars have been detected in globular clusters. Unlike many pulsars in the solar neighborhood, cluster pulsars are known to be predominantly short period ones. Neutron stars are believed to be born with short spin periods ($\lesssim 0.1$ sec) and strong magnetic fields ($10^{12} - 10^{13}$ G). As a neutron star evolves, its rotational energy is released through magnetic dipole radiation which causes deceleration of the spin. Since the spin-down time scales for pulsars with strong magnetic fields are of order 10^8 years while the production of neutron stars in globular cluster must have ceased long time ago, present day population of short period pulsars in clusters must be ‘recycled’ pulsars, which has been spun up by accretion of mass.

Aside from the fact that the abundance of recycled pulsars in globular clusters relative to ordinary stars is far greater than that for solar neighborhood, the cluster pulsars are preferably isolated (as opposed to in a binary system). According to compilation of 558 pulsars by Taylor, Manchester, & Lyne (1993), 19 out of 22 in clusters are *isolated* pulsars while the ratio is only 2 out of 11 in field pulsars. Therefore any theory for the recycled pulsars in globular clusters should explain both the high abundance and high ratio of isolated to binary pulsars.

Proposed mechanisms for producing isolated recycled pulsars in dense stellar regions include close encounters between a neutron star and a main-sequence star leading to a complete or partial disruption of the main-sequence star (Krolik 1984, Lee 1992), and the three-body interactions which can liberate a neutron star in the binary through various ways (see Rappaport, Putney, & Verbunt 1989 for summary). In

the present paper, as a start of the study on the first mechanism, we examine the consequences of close encounters between a neutron star and a main-sequence star.

During a close encounter involving a neutron star, the orbital energy of an incident normal star can be dissipated and stored in its interior by tidal force exerted by a neutron star. Depending on the amount of energy deposited to the stellar envelope, one of the following outcomes are possible: tidal capture of a normal star, or total or partial disruption of the normal star. Based on SPH simulations, Davies, Benz, & Hills (1992) find that encounters involving a main-sequence star of $0.8 M_{\odot}$ can leave a single object for $r_{\min} \lesssim 1.75 R_{MS}$ and detached binaries for $1.7 R_{MS} \lesssim r_{\min} \lesssim 3.5 R_{MS}$, while encounters involving a red giant star leave a compact neutron star-white dwarf binary for $r_{\min} \lesssim 1.8 R_{RG}$ and a detached binary for $1.8 R_{RG} \lesssim r_{\min} \lesssim 2.5 R_{RG}$, where, r_{\min} is the separation at periastron passage. In the present study, while Davies *et al.* concentrated on only one main-sequence star mass, we perform SPH simulations of encounters between a $1.4 M_{\odot}$ neutron star and a main sequence star with a mass in the range between 0.2 and $0.7 M_{\odot}$ for various r_{\min} . This extension will bring a full comparison between simulation and theory, and will eventually provide more realistic information to the study of dynamical evolution of globular clusters.

This paper is organized as follows. In §2, we describe our simulations of stellar encounters, and we discuss the consequences of the encounters based on the simulations in §3. Final section summarizes our major findings.

2. SIMULATION

We adopt an SPH code developed by Monaghan & Lee (1994) for the encounters between a massive black hole and a normal star which is modelled as an $n=3/2$ polytropic sphere. We use 9185 SPH particles to model a main-sequence star and treat the neutron star as a $1.4 M_{\odot}$ point mass that interacts with SPH particles only via gravitational forces. We have chosen main-sequence star mass m to be 0.2, 0.3, 0.5, and $0.7 M_{\odot}$ in our simulations, and the main-sequence stars are assumed to have a linear mass-radius relation (i.e. $R_{MS}/R_{\odot} = m/M_{\odot}$). For R_{MS} of order R_{\odot} and relative velocity at infinity, v_{∞} , of order 10 km s^{-1} , the relative velocity v_{\min} at r_{\min} becomes

$$v_{\min}^2 = \frac{G(M+m)}{r_{\min}} + v_{\infty}^2 \quad (1)$$

$$\simeq \frac{G(M+m)}{r_{\min}}, \quad (2)$$

where M is the mass of the neutron star. This means that v_∞ is not an important parameter in determining the orbit of the star around the neutron star, and in our simulations, v_∞ is always the representative value in globular clusters, 10 km s^{-1} . Therefore we assume that the relative orbit is parabolic for simplicity. We made total of 16 simulations whose input parameters (m and r_{min}) are listed in Table 1.

For the purpose of illustration of the outcome of tidal encounters, we have shown four snapshots of simulation m7p08 in Figure 1. Small dots are the SPH particles, and the curved line is the trajectory that a main-sequence star would follow if it were a point mass. In this figure, the coordinate center is the location of the neutron star. At $t = 1.8 \text{ h}$ (relative to the start of the simulation), the shape of the main-sequence star is already distorted like a Roche lobe which is pointing off the neutron star slightly. At $t = 2.2 \text{ h}$, the SPH particles are spread out in two opposite directions so that the center of mass still reside near the parabolic orbit, and some of the particles from the main-sequence star start to spiral into the neutron star. At $t = 3.3 \text{ h}$, a disk is formed around the neutron star and is still connected to the main body of the main-sequence star which has a long tail of particles with relatively smaller velocities. At $t = 4.2 \text{ h}$, the distortion of main-sequence star has ceased and the main-sequence star is now composed of a sphere with high density and two spiral arms. The disk around the neutron star is expanding in the orbital plane because the particles in the disk has large eccentricities which make them spend much longer time at farther distances than the beginning of the accretion ($t \simeq 3.3 \text{ h}$) when most particles are near their perigees.

3. ANALYSIS

The main purpose of the simulations in this study is to observe how much mass of the main-sequence star can be transferred to the vicinity of (or bound to) the neutron star in the process of close encounter, as a function of m and r_{min} (note that this mass may differ from the actual mass that accretes onto the neutron star surface and consequently spins up the star). Also, we will attempt to predict the future of the main-sequence star remnant, which can be parameterized by its size, r_{min} at the second encounter, and the period of its orbit. The disk formed around the neutron star will be discussed in connection to the spin-up of the neutron star.

3.1. Mass Fractions

To study separately the futures of the disk around the neutron star and of the main-sequence star remnant, it is necessary to judge whether each particle will be bound to the neutron star, remain as a part of the main-sequence star, or escape from the system. Here we employ the following criteria to distinguish among the above three possibilities:

- (A) if $(E_{NS} \leq 0)$ and $(E_{NS} - E_{MS} \leq 0)$, the particle is bound to the neutron star;
- (B) elseif $(E_{MS} \leq 0)$, bound to the main-sequence star;
- (C) else, lost from the system.

The relative energies E_{NS} and E_{MS} are defined as

$$E_{NS} = \frac{1}{2}\mathbf{v}^2 - \frac{GM}{|\mathbf{r}|} \quad (3)$$

$$E_{MS} = \frac{1}{2}(\mathbf{v} - \langle \mathbf{v} \rangle)^2 - \frac{Gm}{|\mathbf{r} - \langle \mathbf{r} \rangle|}, \quad (4)$$

where \mathbf{v} and \mathbf{r} are the velocity and the distance of a particle relative to the neutron star and the brackets denote the averages taken over all SPH particles. Figure 2 is a reproduction of the last snapshot in Figure 1 with three different symbols. Small dots, large dots, and \times 's are the particles that satisfy the conditions A, B, and C, respectively. Note that there are two clear separations between small dots and large dots and between large dots and \times 's. The amounts of mass belonging to each criterion as a function of time for simulation m7p08 are shown in Figure 3. These masses are well defined because each line approaches to an asymptotic value rather quickly.

However, the mass fractions by the above criteria for simulations m2p02 and m7p05 do not approach to asymptotic values, because their r_{\min} 's are so small and the main-sequence star experiences so strong tidal force that the main-sequence star spirals into the neutron star (or, more realistically, the latter spirals into the former) in a relatively short time instead of spending some time on the quite eccentric orbit as an independent object. Thus for these two simulations, it is impossible to distinguish the first encounter and the subsequent one. We do not include these two simulations in the following mass fraction analysis which is limited to the mass fractions of the first encounters only.

The amounts of mass that satisfies criteria A, B, and C are plotted as a function of r_{\min}/R_{MS} in Figure 4 for all simulations except simulations m2p02 and m7p06. Each symbol denotes different main-sequence star mass (see the caption). It is clear that at the same r_{\min}/R_{MS} , heavier main-sequence star loses less fraction of its mass. From the similarity of the curves for each membership, one may expect a parameter that solely determines the mass fractions. For a theoretical approach, we have first tried η of Press & Teukolsky (1977). The quantity η measures the duration of periastron passage, relative to the hydrodynamic

time of the star, and is defined as

$$\eta \equiv \left(\frac{m}{m+M} \right)^{1/2} \left(\frac{r_{\min}}{R_{MS}} \right)^{3/2}. \quad (5)$$

However, it is found that η does not describe the mass fractions in a unified way. Rather, we find that a small alternation to η can make the mass fraction be a function of only one parameter: As shown in Figure 5, the mass fractions of all simulations allign on a single curve if the abscissa of Figure 4 is replaced with a new quantity

$$\eta' \equiv \left(\frac{m}{m+M} \right)^{1/2} \left(\frac{r_{\min}}{R_{MS}} \right)^{3/2} \left(\frac{m}{M} \right)^{1/6}. \quad (6)$$

Theoretical base of the above alternation is as follows: According to Press & Teukolsky (1977), when the relative orbit is assumed to be a parabola, the deposition of orbital energy to stellar oscillations of the star with mass M_1 and the radius R_1 due to the perturbing star with M_2 and R_2 can be expressed by

$$\Delta E = \left(\frac{GM_1^2}{R_1} \right) \left(\frac{M_2}{M_1} \right)^2 \sum_{l=2,3,\dots} \left(\frac{R_1}{r_{\min}} \right)^{2l+2} T_l(\eta), \quad (7)$$

where l is the spherical harmonic index. The dimensionless function $T_l(\eta)$ depends on the structure of the star, and the values of $T_l(\eta)$ for the star with a polytropic index $n = 2/3$ has been calculated by Lee & Ostriker (1986). Then one could expect that the amount of the mass detached from a star during an encounter, Δm , should be related to this ΔE . Furthermore, since the detached mass is a function of η' , ΔE is expected to be a function of η' somehow as well. Indeed we find that $\Delta E/m$ can be well expressed as a function of η' . In Figure 6, $\Delta E/m$'s for three different main-sequence star masses are plotted over η and η' . This comparison clearly shows that $\Delta E/m$ can be expressed more uniformly in terms of η' than just η .

It would be worth while to relate $\Delta m/m$ with $\Delta E/m$. Such relationship can be found in Figure 7. Note that $\Delta m/m$ increases with $\Delta E/m$ linearly until $\Delta m/m \sim 0.1$. After that, it increases quatratically, but the overall tendancy can be approximated to be still linear.

The theoretical quantity ΔE can be obtained in our simulations by finding the difference of the orbital total energies (kinetic + potential) at the start and at the end of the simulation. However, since this calculation is meaningful only when there is almost no mass loss from the main-sequence star, we compare ΔE 's with large η' only. In Figure 8, one can easily see that there is a good agreement between our simulations denoted by several kinds of symbols and the theory denoted by the curves.

3.2. The Main-Sequence Star Remnant

All main-sequence stars in our simulations are captured by the neutron stars and thus will experience subsequent encounters. However, no numerical method has been known to be able to handle such long period of hydrodynamic simulations. For this reason, we have performed the simulations of first encounters only and try to predict the perigee distance at second encounter, $r_{\min,2}$, and the period between first and second perigees, P , from the last dumps of some of our simulations.

To estimate $r_{\min,2}$ and P , we take \mathbf{r} and \mathbf{v} averages for the particles that satisfy the criterion B in the previous subsection. Since the quantities $r_{\min,2}$ and P approach to asymptotic values less quickly than the mass fractions, we have extended simulations m7p08, m7p11, and m7p15 until they show asymptotic values, which are listed in Table 2.

Approximately, simulation m7p15 has twice greater r_{\min} than that of simulation m7p08, but its P is a thousand times longer implying that P has a strong dependency on r_{\min} .

In the above three simulations, $r_{\min,2}$ is about 50 % bigger than r_{\min} . From this fact, the amount of mass stripped during the second encounter, Δm_2 , might be expected to be not as much as that for the first encounter, Δm , but one should remind that the parameter that determines Δm , η' , is a function of R_{MS} too. Since the main-sequence stars are expanded during encounters (see Fig. 9), R_{MS} will have been enlarged at the time of second encounter resulting smaller η' and greater Δm than would be with a constant R_{MS} . Furthermore, as in case of simulation m7p15, even considerable changes in the structure accompany. Also, the rotational angular momentum of the main-sequence star transferred from orbital angular momentum, which is another result of the tidal interaction, may play an important role in determining the amount of mass loss during subsequent encounters. Thus we conclude that the prediction for the fate of the main-sequence star remnant during subsequent encounters is very difficult to obtain from our simulations and that more polished numerical and/or method that can easily handle such a long period of hydrodynamic simulations is necessary for that.

3.3. The Disk

Unlike the binary system where mass transfer to a disk from outside the Roche lobe of a companion is relatively stable, the formation of an accretion disk following a tidal disruption is so abrupt that too much material is put in the disk in a short amount of time. Consequently, the mass accretion rate from the disk onto the neutron star is much higher than the Eddington limit. Verbunt *et al.* (1987) estimated the amount

of accreted mass to be only $(\dot{M}_{Edd}/\dot{M})M_d$ which is insufficient to lead to millisecond periods, where \dot{M}_{Edd} is the mass accretion rate corresponding to the Eddington limit luminosity, \dot{M} the mass accretion rate onto the neutron star, and M_d the disk mass.

The spin period P_s of the neutron star after the accretion is determined by total amount of accreted mass ΔM_{acc} , and the relationship between the final P_s and ΔM_{acc} can be written as

$$\Delta M_{acc} \simeq 0.20f \left(\frac{P_s}{\text{ms}} \right)^{-4/3} M_\odot \quad (8)$$

(Phinney & Kulkarni 1994), where $f \gtrsim 1$ is a factor that depends on the details of the accretion, and the moment of inertia of the neutron star is assumed to be 10^{45}g cm^2 . Until the neutron star reaches its equilibrium period, f remains to be around 3 (Ghosh & Lamb 1992). Further accretion after the equilibrium period does not spin up the star since f has become much higher than 1.

If the steady, thin disk analysis by Ghosh & Lamb (1992) with $f \simeq 3$ is still applicable and if the estimation of mass transferred to the neutron star by Verbunt *et al.* (1987) is valid, the accretion followed by tidal disruption with a rate of $1000 \dot{M}_{Edd}$ may be able to accelerate P_s to $\gtrsim 100$ ms.

On the other hand, if there is a way for all disk material to overcome the Eddington limit and to accrete onto the neutron star's surface, the accretion would be able to accelerate P_s to ~ 1 ms.

The reality will reside somewhere between the above two extreme cases, and the authors will pursue a study on this heavy accretion disk around a neutron star as a next step of the present study.

4. DISCUSSION

We have investigated the consequences of close encounters between a neutron star and a main-sequence star using the SPH method. We have found that the mass fraction stripped from the main-sequence star during the encounter, Δm , is determined only by a single parameter η' in the ranges of m and v_∞ used in our simulations. The orbital energy deposited in the stellar envelope per unit mass, $\Delta E/m$ seems responsible for the mass stripping because it also can be well approximated to be a function of η' .

From simulations with relatively large η' , the core contraction of the main-sequence star remnant has been witnessed as well as the envelope expansion. The radiation from the contracted core will help the envelope expansion and the envelope may not be able to restore itself to the original place.

The mass of the disk formed around a neutron star after an encounter is as much as of order $0.1 M_{\odot}$. If all of this mass could be accreted onto the neutron star's surface, the accretion could accelerate the spin of the neutron star down to 1 ms. However, this kind of heavy accretion disks are subject to high radiation pressure and considerable fraction of the disk is believed to be blown away, which is against the spin-up of the neutron star. The fate of these heavy accretion disks are uncertain and remains to be studied intensively, to explain the high abundance of isolated, recycled pulsars in globular clusters.

We are grateful to Dr. M-G Park for useful conversation on the accretion disk theory. This research was supported in part by the Korea Research Foundation through non-directed research funds in 1993.

Table 1. Simulation Parameters

Simulation	M_{MS} (M_{\odot})	r_{\min} (10^{10} cm)	η	η'	Simulation	M_{MS} (M_{\odot})	r_{\min} (10^{10} cm)	η	η'
m2p02	2	2	0.60	0.44	m5p07	5	7	1.45	1.22
m2p03	2	3	1.11	0.80	m5p09	5	9	2.16	1.78
m2p04	2	4	1.71	1.23	m5p11	5	11	2.86	2.41
m2p05	2	5	2.39	1.72	m7p05	7	5	0.60	0.53
m2p06	2	6	3.14	2.27	m7p08	7	8	1.20	1.07
m3p04	3	4	1.10	0.85	m7p11	7	11	1.94	1.73
m5p06	5	6	1.15	0.97	m7p15	7	15	3.09	2.75

Table 2. Orbital Elements of Selected Simulations

Simulation	r_{\min} (10^{10} cm)	$r_{\min,2}$ ^a (10^{10} cm)	P (h)
m7p08	8	10.9	23
m7p11	11	18.1	210
m7p15	15	22.4	28000

^aPerigee distance at the second encounter

REFERENCES

- Davies M. B., Benz W., & Hills J. G. 1992, *ApJ*, 401, 246
- Ghosh P. & Lamb F. K. 1992, *X-Ray Binaries and Formation of Binary and Millisecond Pulsars*, eds. E. van den Heuvel & S. Rappaport (Dordrecht: Kluwer), 487
- Goodman J. 1988, *ApJ*, 313, 576
- Krolik J. 1984, *ApJ*, 282, 452
- Lee H. M. 1992, *J. Korean Astron. Soc.*, 25, 47
- Lee H. M., & Ostriker, J. P. 1986, *ApJ*, 310, 176
- Monaghan J. J. & Lee H. M. 1994, preprint
- Press W. H. & Teukolsky S. A. 1977, *ApJ*, 213, 183
- Rappaport S., Putney A., & Verbunt F. 1989, *ApJ*, 345, 210
- Taylor J. H, Manchester R. N, & Lyne A. G. 1993, *ApJS*, 88, 529
- Verbunt F., van den Heuvel E. P. J., van Paradijs J., & Rappaport S. A. 1987, *Nature*, 329, 312

Figure not included because of the large file size

You may get this figure at

<http://mercury.es.pusan.ac.kr/papers.html>

Fig. 1.— Four snapshots of simulation m7p08 with $M_{MS} = 0.7 M_{\odot}$ and $r_{\min} = 7 \times 10^{10}$ cm. The hyperbola is the trajectory that the main-sequence star would follow if it were a point mass. All snapshots are in neutron-star-relative coordinates such that the neutron star represented by a cross resides always at (0,0). The axes are in units of R_{MS} .

Figure not included because of the large file size

You may get this figure at

<http://mercury.es.pusan.ac.kr/papers.html>

Fig. 2.— Reproduction of the last snapshot in Figure 1. Small dots are the particles bound to the neutron star, large dots those bound to the main-sequence star, and \times those unbound to the system. For membership criteria, see text. The axes are in units of R_{MS} .

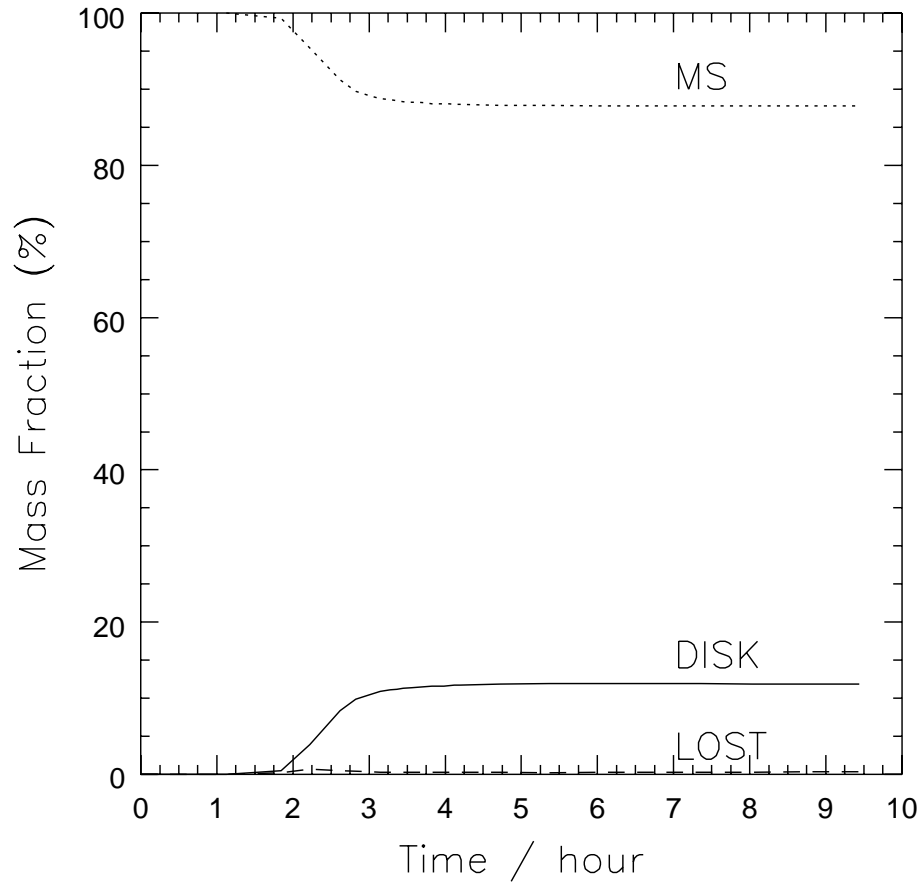


Fig. 3.— Temporal evolution of mass fractions that are bound to the neutron star (DISK), bound to the main-sequence star (MS), and unbound to the system (LOST), for simulation m7p08.

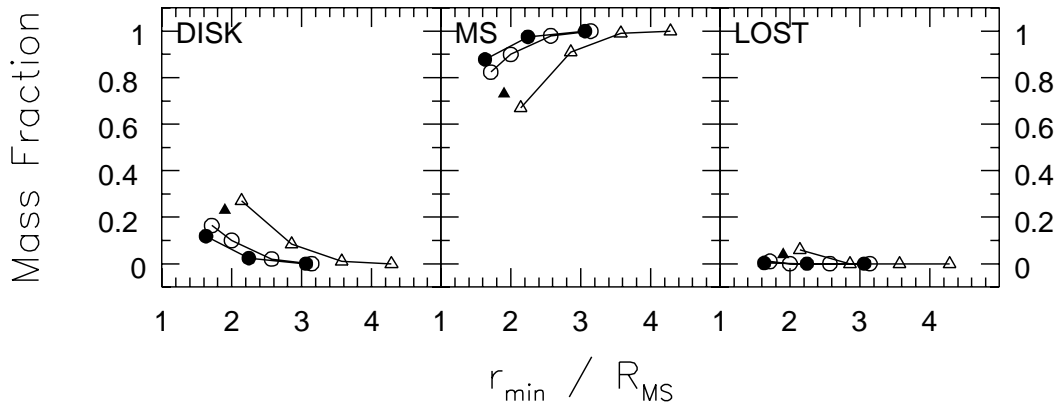


Fig. 4.— Mass fractions that are bound to the neutron star (DISK), bound to the main-sequence star (MS), and unbound to the system (LOST) from the last dumps of all 14 simulations. Filled circles are for $0.7 M_{\odot}$, open circles for $0.5 M_{\odot}$, filled triangle for $0.3 M_{\odot}$, and open triangle for $0.2 M_{\odot}$ main-sequence stars.

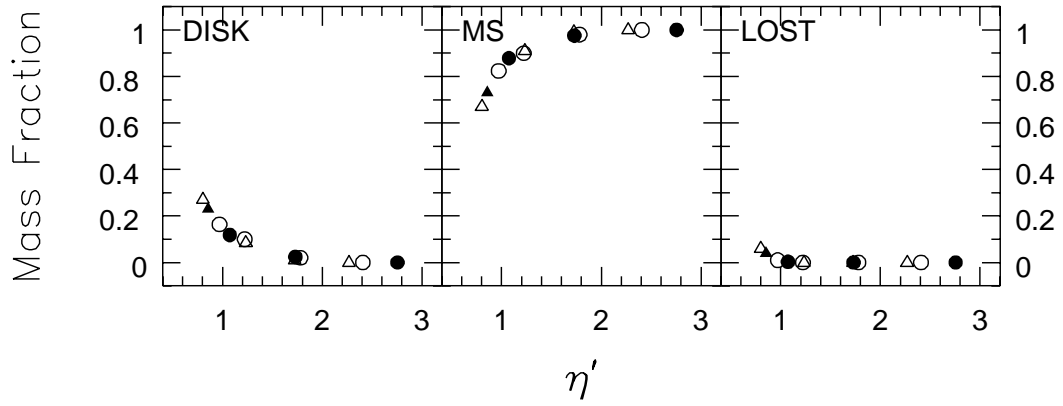


Fig. 5.— Mass fractions. The abscissa of Figure 4 is rescaled for η' now. Symbols are the same as in Figure 4.

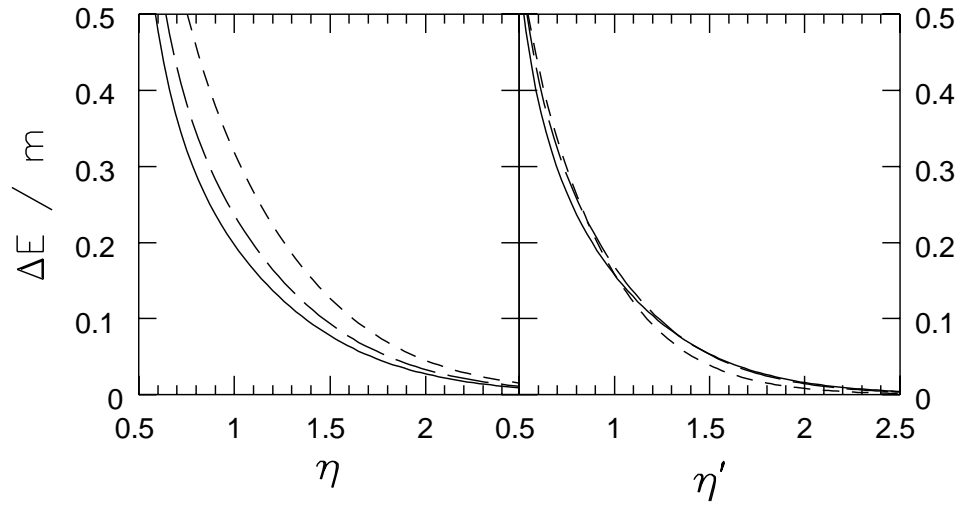


Fig. 6.— Theoretical expectation of orbital energy deposited in the stellar envelope during the first encounter per stellar mass as functions of η and η' for $0.7 M_{\odot}$ (solid), $0.5 M_{\odot}$ (long-dashed), and $0.2 M_{\odot}$ (short-dashed). $\Delta E/m$ in units of GM_{\odot}/R_{\odot} .

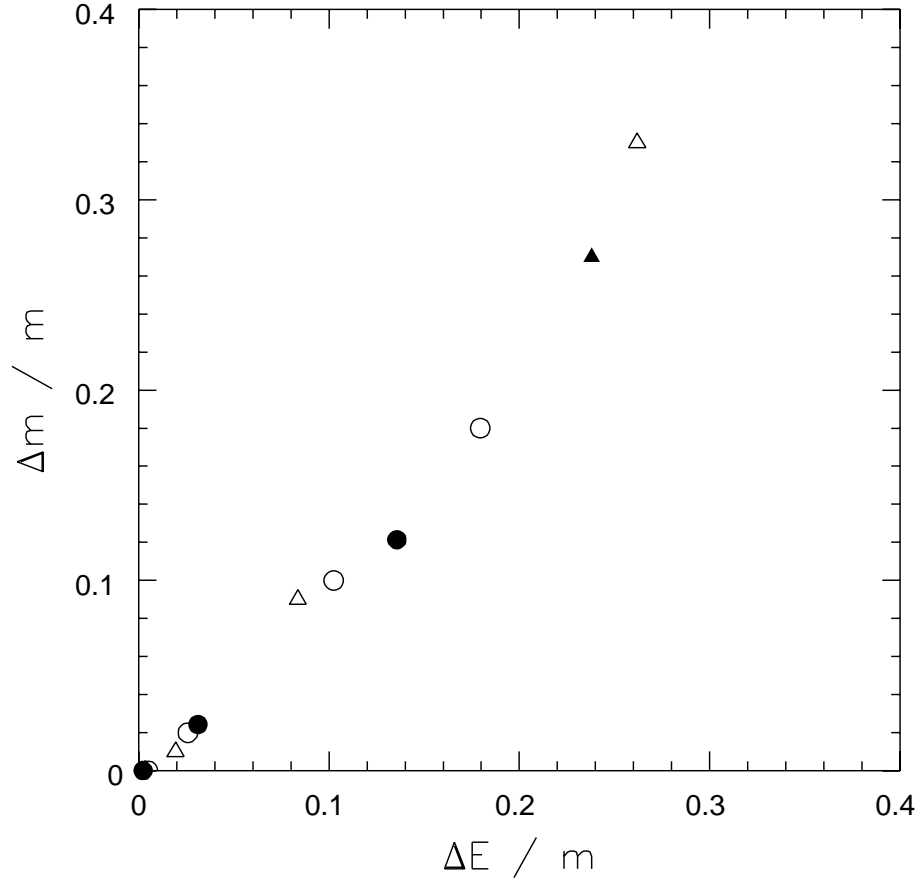


Fig. 7.— The amount of mass stripped per stellar mass versus that of orbital energy deposited in the stellar envelope per stellar mass during the first encounter. $\Delta E/m$ in units of GM_{\odot}/R_{\odot} . Symbols are the same as in Figure 4.

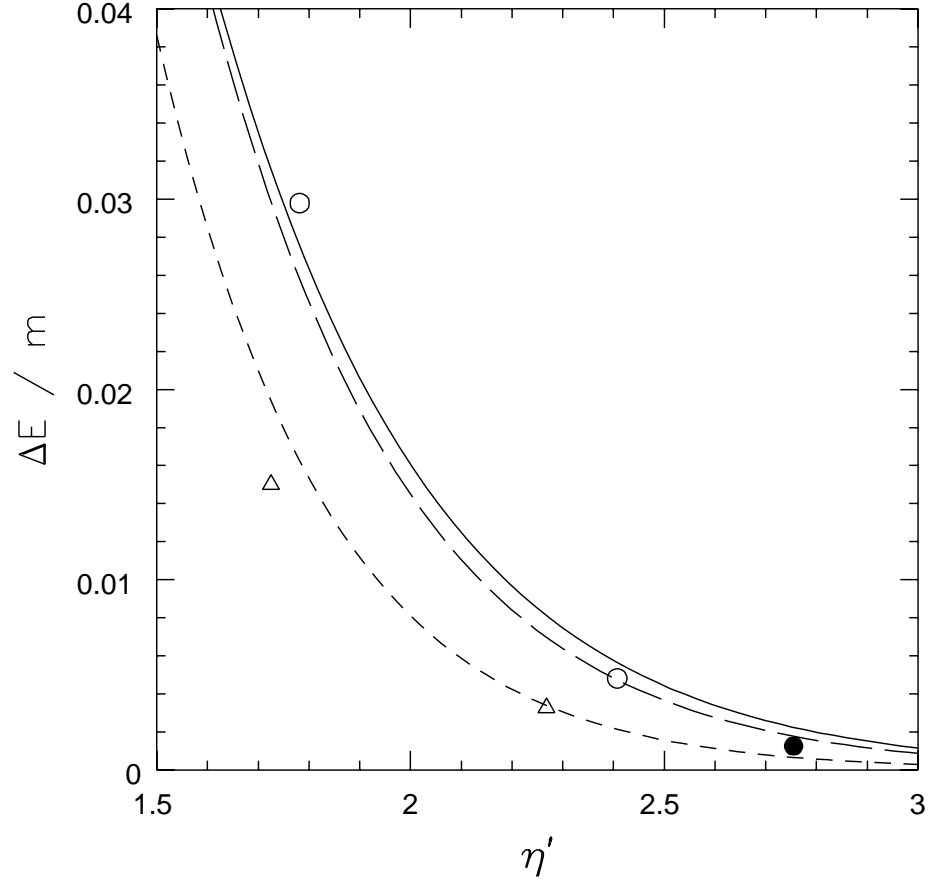


Fig. 8.— Comparison of the amount of orbital energy deposited in stellar envelope per stellar mass between the theory and our simulations. $\Delta E/m$ in units of GM_{\odot}/R_{\odot} . Solid line: $0.7 M_{\odot}$; long-dashed line: $0.5 M_{\odot}$; short-dashed line: $0.2 M_{\odot}$. Symbols are the same as in Figure 4.

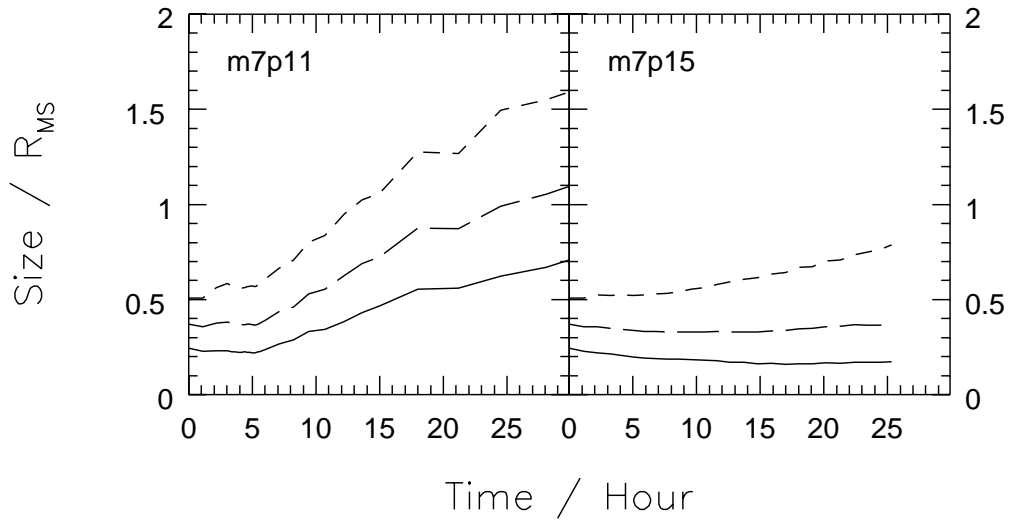


Fig. 9.— Expansion of the main-sequence star remnants of simulations m7p11 and m7p15. Solid lines are the sizes that encompass 25 % of the mass that satisfy the criterion B. Long-dashed lines for 50 % and short-dashed lines for 75 %. The ordinate in units of the original size of the main-sequence star, $0.7 M_{\odot}$.